ELSEVIER

Biochimica et Biophysica Acta 1419 (1999) 207–220

BIOCHIMICA ET BIOPHYSICA ACTA

BBA

www.elsevier.com/locate/bba

Lamellarity of cationic liposomes and mode of preparation of lipoplexes affect transfection efficiency

Nicolaas J. Zuidam, Danielle Hirsch-Lerner, Sharon Margulies, Yechezkel Barenholz *

Department of Biochemistry, The Hebrew University-Hadassah Medical School, P.O. Box 12272, Jerusalem 91120, Israel

Received 16 November 1998; received in revised form 1 March 1999; accepted 26 April 1999

Abstract

Transfection of NIH-3T3 cells by a human growth hormone expression vector complexed with liposomes composed of *N*-(1-(2,3-dioleoyloxy)propyl)-*N*,*N*,*N*-trimethylammonium chloride (DOTAP) with or without helper lipids was studied. The transfection efficiency was dependent on the lamellarity of the liposomes used to prepare the lipoplexes. Multilamellar vesicles (MLV) were more effective than large unilamellar vesicles (LUV) of ~100 nm, irrespective of lipid composition. The optimal DNA/DOTAP mole ratio for transfection was ≤0.5, at which only 10–30% of DOTAP in the lipoplex is neutralized. Prolonged incubation time of lipoplexes before addition to cells slightly decreased the level of transfection. A major influence on the lipofection level was found when the mode of lipoplex preparation was varied. Mixing plasmid DNA and DOTAP/DOPE (1:1) LUV in two steps instead of one step resulted in a higher lipofection when at the first step the DNA/DOTAP mole ratio was 0.5 than when it was 2.0. Only static light-scattering measurement, which is related to particle size and particle size instability, revealed differences between the lipoplexes as a function of lamellarity of the vesicles (MLV or LUV), mixing order, and number of mixing steps. Other physical properties of these lipoplexes were dependent only on the DNA/DOTAP mole ratio, i.e. the extent of DOTAP neutralization (as monitored by ionization of the fluorophore 4-heptadecyl-7-hydroxycoumarin) and the extent of defects in lipid organization (as monitored by level of exposure of the fluorophore 1-(4-trimethylammoniumphenyl)-6-phenyl-1,3,5-hexatriene to water). The secondary and tertiary structure of DNA in lipoplexes was evaluated by circular dichroism spectroscopy. The results of this study point out that the structure of lipoplexes should be physicochemically characterized at two different levels: the macro level, which relates to size and size instability, and the micro level, which relates to the properties described above which are involved in the intimate interaction between the plasmid DNA and the lipids. At the micro level, all parameters are reversible, history-independent and are determined by DNA/DOTAP mole ratio. On the other hand, the macro level (which is the most important for transfection efficiency) is history-dependent and not reversible.

Keywords: Fluorescence; DNA; Human growth hormone; Gene delivery; Gene therapy

Abbreviations: DOPC, 1,2-dioleoyl-*sn*-glycero-3-phosphatidylcholine; DOPE, 1,2-dioleoyl-*sn*-glycero-3-phosphatidylethanolamine; DOTAP, *N*-(1-(2,3-dioleoyloxy)propyl)-*N*,*N*,*N*-trimethylammonium chloride; HC, 4-heptadecyl-7-hydroxycoumarin; HEPES, *N*-(2-hydroxyethyl)piperazine-*N*′-(2-ethanesulfonic acid); hGH, human growth hormone; LUV, large unilamellar vesicles; MLV, multilamellar vesicles; TMADPH, 1-(4-trimethylammoniumphenyl)-6-phenyl-1,3,5-hexatriene

* Corresponding author. Fax: +972-2-641-1663; E-mail: yb@cc.huji.ac.il

0005-2736/99/$ – see front matter
PII: S0005-2736(99)00069-3

1. Introduction

Spontaneously formed lipoplexes, which are complexes formed upon mixing of DNA and liposomes containing positively charged cationic lipids, have been widely used to transfect mammalian cells in vitro and in vivo [1–5]. Lipoplexes probably enter cells mainly by adsorptive endocytosis [2,3,6–9]. The intracellular route is not yet clear; however, it is clear that only a small fraction of the lipoplexes is able to escape lysosomal degradation and to end up in the nucleus [7,8]. The transfection ability of lipoplexes in vitro depends on many parameters, such as their physicochemical characteristics, type of cells, and incubation conditions [2–4]. In spite of all the currently available relevant information, the rational way to optimize lipofection in vivo is still unclear.

The thermodynamic driving force for the spontaneous formation of the lipoplexes is the lowering in total free energy of the lipoplexes when compared with those of the liposomes and the DNA. The main forces which contribute to the total free energy of the lipoplexes include the electrostatic forces, elastic (bending and stretching) forces, and for liposomes of more than one component, also contributions of mixing or demixing of lipids. In general, in order to obtain lipoplexes spontaneously, the lowering of electrostatic free energy due to neutralization of the positively charged membranes by the negatively charged nucleic acids must be larger than the elastic energetic cost involved in the lipid molecule adapting to the lipoplex geometry [10,11]. Lipoplexes exhibit a large degree of polymorphism, which is dependent on the specific lipid composition, on the charge ratio between the cationic lipid and the DNA (L^+/DNA^-), and on the medium composition [2–4,12]. The system of mixtures of cationic liposomes and DNA can be described by phase diagrams, which in principal contain three regions: (1) in large excess of cationic lipids there is coexistence of liposomes and lipoplexes; (2) in large excess of DNA, there is coexistence of naked DNA and lipoplexes; and (3) the in-between region, in which only lipoplexes exist. However, the properties of the lipoplexes throughout the phase diagram are not necessarily identical.

From the vast amount of studies performed on lipofection over the last decade (reviewed in [1–5]) it is clear that even in vitro (and more so in vivo) the lipofection process is multifactorial. Some of the factors involved are external and related to the type of cells and lipofection medium. Other factors are intrinsic and directly related to the physicochemical properties and mode of lipoplex preparation. The present study is aimed to better understand the role of the intrinsic lipoplex-related factors. Therefore, in this study, only one type of cell (NIH-3T3), identical medium, and one cationic lipid (*N*-(1-(2,3-dioleoyloxy)propyl)-*N*,*N*,*N*-trimethylammonium chloride, DOTAP) were used. The lipoplex composition variables which were investigated are the presence and type of helper lipid, the lamellarity of the liposomes, the DOTAP/DNA mole ratio, and the mode of lipoplex preparation.

2. Materials and methods

2.1. Materials

The plasmid pS16-GH, a 4.8-kbp plasmid containing a gene coding for human growth hormone (hGH), was a kind gift of Dr. O. Meyuhas of our department (see for further details [13]). DOTAP, DOPE, and DOPC were obtained from Avanti Polar Lipids (Alabaster, AL, USA). These and all other chemicals were of analytical grade or better. Double-distilled water was used.

2.2. DNA preparation

Plasmid pS16-GH was grown in *Escherichia coli* and isolated using a QIAGEN Mega Plasmid Kit (QIAGEN, Hilden, Germany) according to the instructions of the kit's manufacturer. The final concentration of plasmid DNA in 20 mM HEPES buffer (pH 7.4) was quantified by organic phosphate determination [14]. The concentration of DNA in the present study is expressed as equivalent concentration of phosphate. Agarose gel (1%) electrophoresis [15] showed that the plasmid DNA was mainly in a supercoiled form and free from chromosomal DNA or RNA. UV-spectroscopy [15] showed no presence of contamination of proteins in the several DNA batches: the ratio of absorbance at 260 nm to that at 280 nm was about 1.8–1.9, and the absorbance at 320 was negligible.

2.3. Liposome preparation

Appropriate mixtures of lipids were dissolved in methanol/chloroform (1:1) (v/v) in a round-bottom flask. An appropriate amount of the fluorophore 4-heptadecyl-7-hydroxycoumarin (HC) dissolved in tetrahydrofuran or the fluorophore 1-(4-trimethylammoniumphenyl)-6-phenyl-1,3,5-hexatriene (TMADPH) dissolved in tetrahydrofuran/ethanol (1:1) (v/v) was sometimes added to this mixture to give a final probe/DOTAP mole ratio of 1:400 or 1:200, respectively. After evaporation of the organic solvent by rotary evaporation, the lipids were again dissolved in *tert*-butanol and this mixture was freeze-dried for at least 3 h under reduced pressure. The hydration of the lyophilized 'cake' was performed with 20 mM HEPES (pH 7.4) and vortexed for several minutes. If necessary, liposomes were downsized using the extrusion system LiposoFast (AVESTIN, Ottawa, ON, Canada; see [16]) 11 times through 0.4-μm- and 11 times through 0.1-μm-pore-size filters (Poretics, Livermore, CA, USA), successively. In all batches, unless mentioned otherwise, the concentration of each type of lipid was 20 mM.

2.4. Fluorescence and static light-scattering measurements

Cationic liposomes were diluted in 3 ml of 20 mM HEPES buffer (pH 7.4) to a concentration of 4×10^{-5} M of the cationic lipid. The measurements were performed on an LS50B luminescence spectrometer (Perkin-Elmer, Norwalk, CT, USA) while stirring at ambient temperature. The advantages of HC and its measurement as a pH- and potential-sensitive fluorescent membrane probe are discussed in a previous paper [17]. Briefly, fluorescence intensity of HC was measured at excitation wavelengths of 330 (the pH-independent isosbestic point) and 380 nm, using a constant emission wavelength of 450 nm (bandwith 5 nm). The use of the isosbestic point enabled us to correct for differences in fluorescence intensities due to small differences in HC concentration or aggregation of the lipoplexes. The use of TMADPH and the measurement of its fluorescence intensity was performed as described before [18]. Briefly, fluorescence intensity of TMADPH was measured at excitation wavelength 360 nm and emission wavelength 430 nm. Static light-scattering (also referred to as turbidity) of the same sample was obtained on the same spectrofluorometer using both excitation and emission wavelength at 600 nm (bandwidths 2.5 nm and an attenuation of 1% when the measurements were done with TMADPH-labeled liposomes).

2.5. Transfection of cells

Lipoplexes were made by mixing an appropriate amount of cationic liposomes from a parent solution containing 1×10^{-3} M cationic lipid with 1×10^{-4} M plasmid pS16-GH in 20 mM HEPES buffer (pH 7.4). If not indicated otherwise, these lipoplexes were incubated 15 min at ambient temperature. Then, an aliquot of 50 μl of the DNA–lipoplexes (containing 5 nmol ($\approx$1.5 μg) DNA) was added to a well of a 24-well plate containing 40–60% confluent NIH-3T3 cells with 1.0 ml fresh cell medium. The cell medium consisted of DMEM with 0.2 mM L-glutamine, 10% (w/w) fetal calf serum, 1 mg/ml penicillin, and 100 U/ml streptomycin (all obtained from Biological Industries, Beit Haemek, Israel). After incubation in a 5% CO_2-incubator at 37°C for 24 h (the cells were 90–100% confluent), the concentration of hGH in the supernatant of the wells was estimated by using a radioimmunoassay for hGH (Nichols Institute, San Juan Capistrano, CA, USA).

2.6. Circular dichroism spectroscopy

Circular dichroism (CD) spectra were obtained using a Jobin–Yvon CD6 instrument (ISA, Longjumeau, France). A circular quartz cell with a path length of 1 cm was used. The integration time was set to 2 s, and the slit to 2 nm. Each measurement was the average of 4 repeated scans in steps of 2 nm at 20°C. First, the CD spectrum of 20 mM HEPES buffer was measured. Then, the CD spectrum of 'free' plasmid at a plasmid DNA concentration of 4×10^{-5} M (based on phosphate content) was measured. Afterwards, an appropriate amount of liposomes was added to the sample. After 5 min incubation at ambient temperature, the CD spectrum of the DNA–lipid complex was measured. Then, an appropriate amount of liposomes or DNA was added and the CD spectrum of this sample was measured again.

The spectrum of the buffer solution of each sample was substracted from the spectrum of each sample.

3. Results

3.1. Cationic liposome-mediated transfection

In this study, NIH-3T3 cells were transfected with the plasmid pS16-GH, which contains a gene coding for human growth hormone (hGH). The level of hGH produced after incubation with 'naked' plasmid DNA is negligible (<0.1 ng/ml), as was also observed in control experiments with cationic liposomes alone, buffer, or nothing added to the cells. Fig. 1 shows the results of the transfection of NIH-3T3 cells when plasmid DNA was added to non-sized, multilamellar vesicles (0.5–1.0 μm in size) in the DNA/DOTAP charge ratio range of 0.2–2.0. Using DOTAP/DOPE (1:1) MLV, the highest lipofection efficiency was obtained when the DNA/DOTAP ratio was 0.2. The same trend was observed upon using 100% DOTAP MLV. However, for 100% DOTAP at the higher DNA/DOTAP charge ratios the lipofection efficiency was lower. A different pattern was observed when DOTAP/DOPC (1:1) MLV were used for the lipofection. The optimal DNA/DOTAP ratios were at 0.5 and 1.0, while at a lower or higher ratio the lipofection efficiency decreased. For MLV,

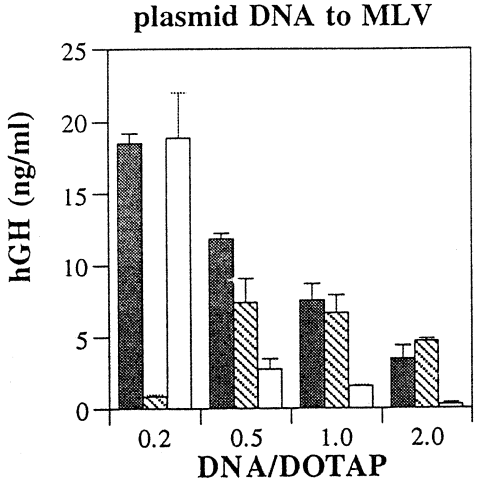

Fig. 1. Amount of hGH in the supernatant of NIH-3T3 cells after addition of lipoplexes made by mixing plasmid DNA with MLVs composed of DOTAP/DOPE (1:1) (gray bars), DOTAP/DOPC (1:1) (hatched bars), or 100% DOTAP (white bars).

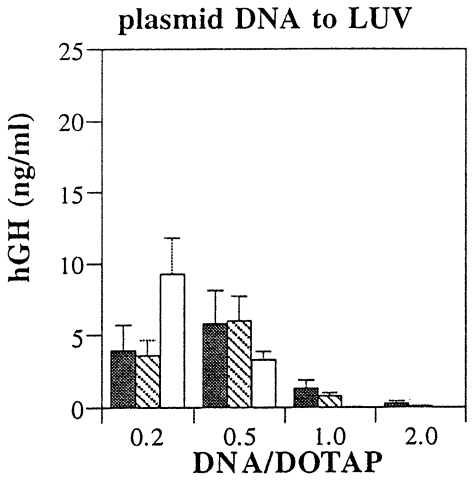

Fig. 2. Amount of hGH in the supernatant of NIH-3T3 cells after addition of lipoplexes made by mixing plasmid DNA with LUVs composed of DOTAP/DOPE (1:1) (gray bars), DOTAP/DOPC (1:1) (hatched bars), or 100% DOTAP (white bars).

the dependency of transfection on DNA/DOTAP ratio was in the order 100% DOTAP $\approx$ DOTAP/DOPE (1:1) $\gg$ DOTAP/DOPC (1:1).

Downsizing of the cationic MLV, prior to their complexation with DNA, to unilamellar vesicles (LUV) of about 100 ± 20 nm and adding the DNA to the LUV resulted in lower transfection than when MLV were used for lipoplex preparation (compare Fig. 2 with Fig. 1). For all the LUV DNA/DOTAP ratios studied, the best results were obtained when the LUV composition consisted of DOTAP/DOPE (1:1) or DOTAP/DOPC (1:1) at the DNA/DOTAP mole ratio of 0.5; using 100% DOTAP LUV resulted in lower transfection. The exception is DOTAP/DNA ratio of 0.2, where lipofection efficiency was the highest without the helper lipids (100% DOTAP LUV). Another observation is that the dependence of DNA/DOTAP ratio of all three lipid compositions was higher when LUV rather than MLV were used for lipoplex preparation.

To gain further information about the impact of the preparation procedure on the lipofection efficiency, plasmid DNA–DOTAP/DOPE (1:1) lipoplexes were prepared in three additional ways: (1) the lipoplexes were prepared by adding DNA to LUV and incubated for longer periods of time prior to addition to the cells; (2) the mixing order was reversed (adding LUV to plasmid DNA); and (3) the lipoplexes were made in two steps instead of

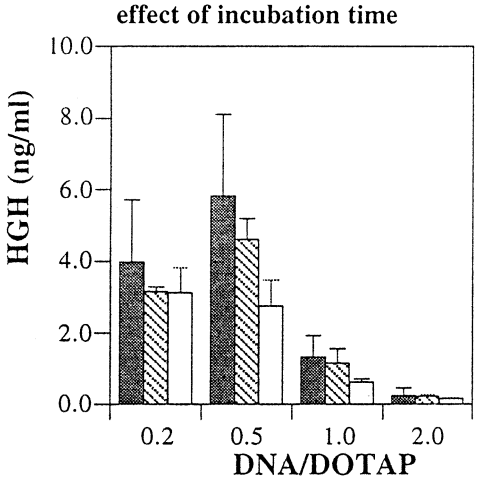

Fig. 3. Amount of hGH in the supernatant of NIH-3T3 cells after addition of DNA–cationic lipid complexes made by mixing plasmid DNA with MLVs composed of DOTAP/DOPE (1:1) and incubated 15 min (gray bars), 3 h (hatched bars) and 24 h (white bars) before addition to the cells.

one. The following results were obtained: (1) a prolonged incubation time of the lipoplexes prior to transfection resulted in some decreases in transfection efficiency of DNA–DOTAP/DOPE (1:1) lipoplexes (Fig. 3); (2) with DOTAP/DOPE (1:1) LUV the addition of LUV to DNA resulted in a better lipofection than the addition of DNA to LUV at all DNA/DOTAP ratios; only at a DNA/DOTAP ratio of 1.0 this superiority was statistically significant (Fig. 4); and (3) mixing plasmid DNA and DOTAP/DOPE (1:1) LUV in two steps instead of one also resulted in different transfection efficiencies (Fig. 4); a higher transfection efficiency was found when the DNA/DOTAP ratio after the first step was 0.5 than when the DNA/DOTAP ratio after the first step was 2.0. This was especially striking when these ratios were at the final DNA/DOTAP ratio of 2.0. The observation was made that in the case of lipoplexes with an initial DNA/DOTAP ratio of 2.0 (conditions of very low transfection) followed by reducing the DNA/DOTAP ratio at the second step to 0.5, the transfection efficiency was almost identical to that obtained at one-step mixing at a DNA/DOTAP ratio of 0.5.

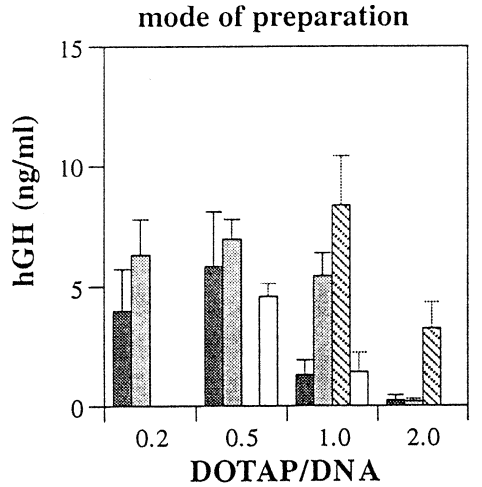

Fig. 4. Amount of hGH in the supernatant of NIH-3T3 cells after addition of lipoplexes of indicated DNA/DOTAP ratios made by mixing in one step plasmid DNA added to DOTAP/DOPE (1:1) LUVs (dark gray bars) or DOTAP/DOPE (1:1) LUVs to plasmid DNA (hatched bars), or by mixing in two steps in such a way that the DNA/DOTAP ratio was 0.5 (light gray bars) or 2.0 (white bars) after the first step.

3.2. *Physical characteristics of DNA–DOTAP/DOPE (1:1) lipoplexes*

Appropriate amounts of plasmid DNA were mixed with cationic DOTAP/DOPE (1:1) liposomes containing the fluorophore HC, which is a weak acid, and the change in its degree of dissociation in the lipid layers was monitored with time by measuring

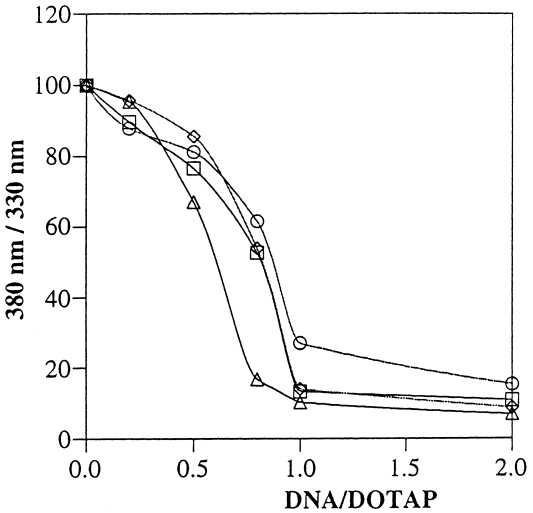

Fig. 5. Ratio of the fluorescence intensities of HC emission at 450 nm as a result of excitation at 380 and 330 nm (HC 380/330 fluorescence ratio) in the lipoplexes upon mixing of plasmid DNA and DOTAP/DOPE (1:1)–liposomes after 15 min incubation. The lipoplexes were made by adding plasmid DNA to MLV (◇), MLV to plasmid DNA (△), plasmid DNA to LUV (○), or LUV to plasmid DNA (□).

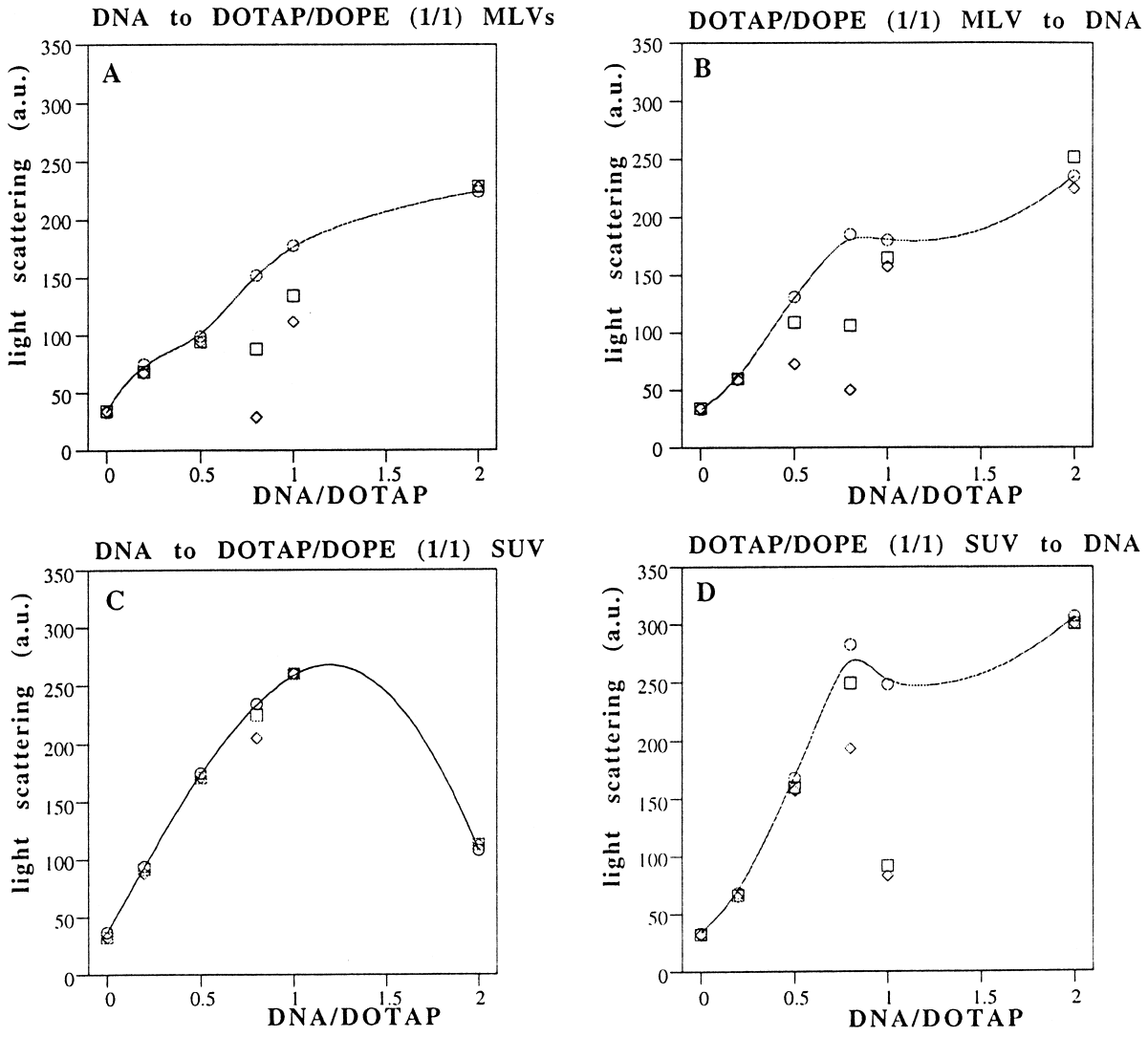

Fig. 6. Static light-scattering measured by the spectrofluorometer (excitation = emission = 600 nm) of lipoplexes after 5 min (○), 15 min (□), and 30 min (◇) incubation. The lipoplexes were made by mixing plasmid DNA with MLVs (A), MLVs with plasmid DNA (B), plasmid DNA with LUVs (C), or LUVs with plasmid DNA (D).

the value of the ratio of the excitation intensities at the pH-dependent 380 nm and at the pH-independent isosbestic point of 330 nm (380/330 fluorescence ratio), using 450 nm as the emission wavelength. In a previous paper [19], we showed that there is almost a 1:1 correlation between the amount of HC in the dissociated form and the level of charge density of the cationic lipids in the dispersions used here.

Fig. 5 shows the change in the 380/330 fluorescence ratio of HC in DOTAP/DOPE (1:1) liposomes (MLV or LUV) upon mixing with different amounts of plasmid DNA. The plasmid DNA was added to DOTAP/DOPE (1:1) MLV or DOTAP/DOPE (1:1) LUV, or the liposomes were added to the plasmid DNA. The decrease in the HC 380/330 fluorescence ratio was instantaneous upon DNA–liposome mixing, and hardly changed with time for the first 15 min (see Fig. 7). No significant change in the absolute intensity of the fluorescence at the isosbestic point (excitation at 330 nm) was observed (except in the cases of severe aggregation of the DNA–cationic lipid lipoplexes, see Fig. 7C). The reduction of HC 380/330 fluorescence ratio in DNA–DOTAP/DOPE (1:1) lipoplexes depended only on the DNA/DOTAP ratios; neither the vesicle lamellarity nor sequence of mixing affected it. The dissociation degree of HC as a

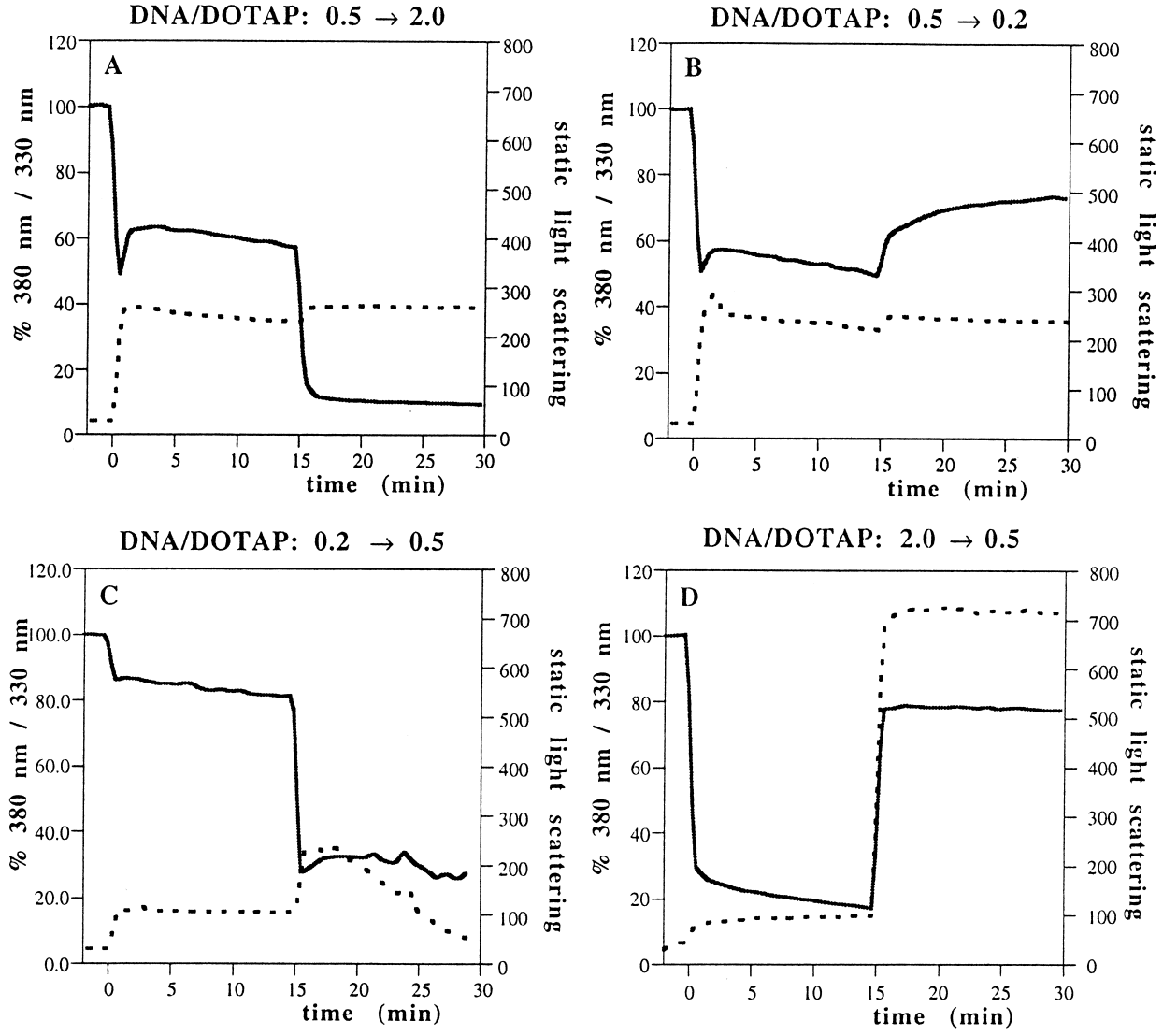

Fig. 7. Change in the static light-scattering of the lipoplexes (broken lines) and in the HC 380/330 fluorescence ratio (unbroken lines) in the cationic membranes upon mixing plasmid DNA with LUV composed of DOTAP/DOPE (1:1). The lipoplexes were made as follows. (A) At time 0, 60 nmol plasmid DNA was added to 240 nmol DOTAP/DOPE (1:1) LUV containing HC. After 15 min, 180 nmol plasmid DNA was added to this lipoplex. (B) At time 0, 60 nmol plasmid DNA was mixed with 240 nmol DOTAP/DOPE (1:1) LUV. After 15 min, 360 nmol DOTAP/DOPE (1:1) LUV (without HC) was added to this lipoplex. (C) At time 0, 24 nmol plasmid DNA was added to 240 nmol DOTAP/DOPE (1:1) LUV containing HC. After 15 min, 36 nmol plasmid DNA was added to this lipoplex. (D) At time 0, 240 nmol plasmid DNA was mixed with 240 nmol DOTAP/DOPE (1:1) LUV. After 15 min, 720 nmol DOTAP/DOPE (1:1) LUV (without HC) was added to this lipoplex. The final volume of all samples was 3 ml.

function of the DNA/DOTAP mole ratio was an inverse sigmoid, and reached a plateau of 80–90% reduction for all four combinations used here at a DNA/DOTAP ratio of 1.0 (see Fig. 5). Static light-scattering was, in contrast to the HC-fluorescence measured in parallel, described in Fig. 5, dependent on type of vesicles used (MLV or LUV) and on sequence of addition (DNA to liposomes or liposomes to DNA) (see Fig. 6). In general, values for static light-scattering increased almost linearly with increasing amounts of plasmid DNA added to a constant amount of liposomes up to a DNA/DOTAP ratio of 1.0, irrespective of order of mixing and lamellarity. Above the ratio of 1.0, the order of mixing and the lamellarity differ in their static light-scattering. Interestingly, plasmid DNA mixing with LUV

Table 1
The TMADPH relative fluorescence intensity (F/F_o) and the specific turbidity (T/T_o) in DOTAP/DOPE liposomes upon lipoplex formation

[Lipid] (mM)	Ratio DNA^-/L^+	F/F_o	T_o	Specific turbidity (T/T_o)
0.08	1.4	1.34 ± 0.04	0.37 ± 0.26	3.97 ± 0.39
0.26	0.44	0.57 ± 0.06	1.07 ± 0.11	9.48 ± 1.35
0.78	1.4	1.55 ± 0.03	2.60 ± 0.38	4.68 ± 1.34
0.78	0.44	0.50 ± 0.01	2.74 ± 0.11	5.84 ± 0.73
0.08 → 0.26	1.4 → 0.44	0.53 ± 0.08	0.52 ± 0.08	1.35 ± 0.67
0.78	0.44 → 1.4	1.59 ± 0.15	2.72 ± 0.08	9.54 ± 0.15

F_o and T_o are the fluorescence intensity and the static light-scattering of the liposomes before the addition of DNA, respectively.

resulted in somewhat higher values of the static light-scattering (per identical lipid concentration) than plasmid DNA mixing with MLV. Also, static light-scattering decreased when increasing amounts of plasmid DNA were added to DOTAP/DOPE (1:1) LUV, while it slightly increased when increasing amounts of DOTAP/DOPE (1:1) LUV were added to plasmid DNA or when DOTAP/DOPE (1:1) MLV were used. Decrease with time in the light-scattering values of the lipoplexes with DNA/DOTAP mole ratios of 0.5–1.0 indicated aggregation (as could also be clearly seen by eye).

Fig. 7 demonstrates typical examples of the changes in static light-scattering and dissociation degree of HC in DNA–DOTAP/DOPE (1:1) lipoplexes with time during two-step mixing of plasmid DNA and DOTAP/DOPE (1:1) LUV. Fig. 7A and B show the parallel changes in static light-scattering and dissociation degree of HC of DNA–DOTAP/DOPE (1:1) lipoplexes when the DNA/DOTAP = 0.5 after the first step, and 2.0 (Fig. 7A) or 0.2 (Fig. 7B) after the second step. The first addition of plasmid DNA to DOTAP/DOPE (1:1) LUV resulted in an instant decrease in the HC 380/330 nm fluorescence ratio and an instant increase in the light-scattering. In general, these parameters did not further change with time (except after longer times, when the DNA–cationic lipoplexes aggregated (at DNA/DOTAP ratios between 0.5 and 1.0; see Figs. 5 and 6 and [19]). Further addition of plasmid DNA to the DNA–DOTAP/DOPE (1:1) lipoplexes (final DNA/DOTAP ratio = 2.0) resulted in a further decrease of the 380/330 nm ratio to the expected value (~85% reduction [19]), and in only a minimal increase in static light-scattering (Fig. 7A). When the second step was adding DOTAP/DOPE (1:1) LUV to a final DNA/DOTAP ratio = 0.2, the HC 380/330 fluorescence ratio increased (although to a lesser degree than expected from [19]) (compare Fig. 7B with Fig. 5 and the first step in Fig. 7C). The static light-scattering was minimally increased, but definitely not reduced to the expected level (compare with Fig. 6 or Fig. 7C). Fig. 7C shows the results of the preparation of this latter lipoplex at a DNA/DOTAP mole ratio of 0.2 in one step; interestingly, the values for the dissociation degree of HC and especially the static light-scattering differ from those obtained reaching the DNA/DOTAP ratio of 0.2 in two steps (Fig. 7B). A second addition of DNA to a final DNA/DOTAP ratio of 0.5 (Fig. 7C) resulted in a dissociation degree of HC similar to the one observed after getting the DNA/DOTAP ratio 0.5 in one step (see that value after the first step in Fig. 7A), and in a gradual decrease in static light-scattering with time caused by a decrease in the number of lipoplexes due to flocculation of the DNA–DOTAP/DOPE (1:1) lipoplexes (as could also be clearly seen by eye). The absolute fluorescence values of HC followed a similar decrease with time. However, as shown in Fig. 7C, the HC 380/330 nm fluorescence ratio in the flocculating lipoplexes remained constant. Fig. 7D shows the results of the reverse of the experiment of Fig. 7A. The dissociation degree of HC in DNA–DOTAP/DOPE (1:1) lipoplexes of a DNA/DOTAP ratio of 2.0 was almost identical comparing addition of DNA in one step and in two steps (compare the first addition of the curve in Fig. 7D with the final stage of Fig. 7A). However, this similarity was not found with the static light-scattering which was lower (half) when a DNA/DOTAP ratio of 2.0 was reached after one step (Fig. 7D) than when this ratio was reached in two steps. Further addition of DOTAP/DOPE

(1:1) LUV resulted in DNA–DOTAP/DOPE (1:1) lipoplexes of a DNA/DOTAP ratio of 0.5 and in a large (≈7-fold) increase in static light-scattering. Again, the dissociation degree of HC in these lipoplexes made in two steps was similar to the one made in one step (compare Fig. 7D and A), in contrast to the values of the static light-scattering. To sum up, the comparison of HC dissociation and static light-scattering with lipoplexes, obtained after one or two steps of DNA mixing with cationic DOTAP/DOPE (1:1) LUV, reveals that HC dissociation was reversible and dependent only on the final DNA/DOTAP mole ratio. On the other hand, the static light-scattering was dependent on the history of the mode of lipoplex preparation, having the DNA/DOTAP mole ratio of 0.5 as a dominant factor in determining the static light-scattering.

Lipoplexes formed from DOTAP/DOPE (1:1) LUV and DNA at mole ratios of 0.44 and 1.4 were studied for the effect of the history of reaching these two DNA/DOTAP mole ratios (Table 1). Similar fluorescence quenching of TMADPH was observed at the DNA/DOTAP ratio of 0.44 with 0.26 and 0.78 mM lipid, indicating increased exposure of the probe to water due to membrane defects [18]. In contrast, a similar fluorescence enhancement of TMADPH was measured at a DNA/DOTAP mole ratio of 1.4 at 0.08 and 0.78 mM lipid, indicating reduced probe exposure to water due to dehydration of the lipid assembly [18]. For both DNA/DOTAP ratios the effect was lipid-concentration independent when the DNA/DOTAP ratio was changed from 1.4 to 0.44 (lipoplex preparation in two steps), the fluorescence quenching was as expected after preparation of lipoplexes with DNA/DOTAP ratio 0.44 in one step, but the specific turbidity was much smaller (1.35) than the value of lipoplexes at this DNA/DOTAP mole ratio prepared in one step (9.48 or 9.54 at different lipid concentrations). When the DNA/DOTAP mole ratio was shifted from 0.44 to 1.4, at the second mixing step, an increase in the fluorescence intensity was observed, as expected, for lipoplexes with a DNA/DOTAP mole ratio of 1.4. However, the static light-scattering remained at the higher value expected for lipoplexes with a DNA/DOTAP mole ratio of 0.44. These data support those described in Fig. 7. Thus, variables related to the intimate interactions between DNA and lipids are dependent mainly on

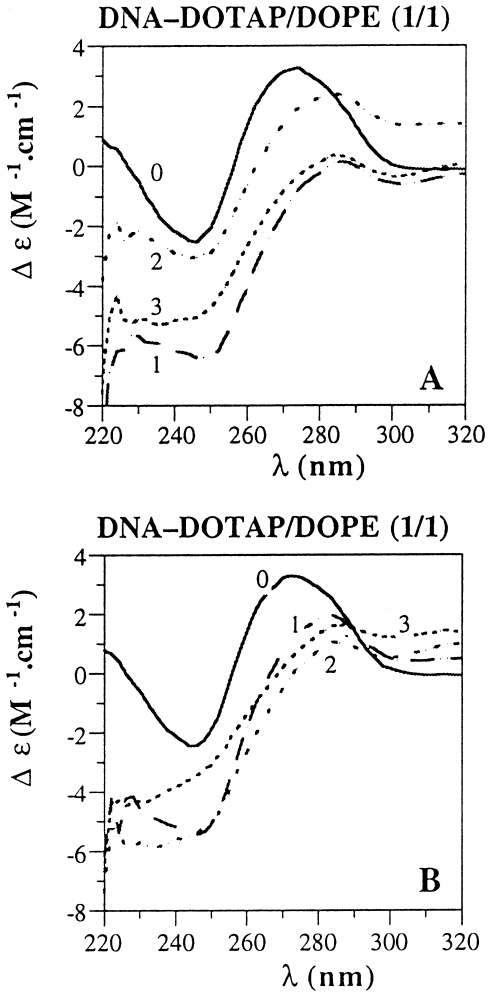

Fig. 8. CD spectra of DNA–DOTAP/DOPE (1:1) complexes upon addition of DOTAP/DOPE (1:1) LUV. (A) Complex at a DOTAP/DNA mole ratio of 1.5 (curve 1), followed by addition to this complex of plasmid DNA to a DOTAP/DNA mole ratio of 0.75 (curve 2), and followed by addition of DOTAP/DOPE (1:1) LUV to a DOTAP/DNA mole ratio of 1.5 (curve 3). (B) Complex at a DOTAP/DNA mole ratio of 3.0 (curve 1), followed by addition to this complex of plasmid DNA to a DOTAP/DNA mole ratio of 1.5 (curve 2), and followed by addition of DOTAP/DOPE (1:1) LUV to a DOTAP/DNA mole ratio of 3.0 (curve 3). The CD spectra of 'free' plasmid DNA are also given in A and B (curve 0).

DNA/DOTAP ratio, while size and size instability are history-dependent. Changes in TMADPH fluorescence intensity, when combined with changes in specific turbidity (turbidity per mole lipid), are indicative of the degree of size instability due to packing defects in the lipid assembly [18]. Table 1 summarizes these two variables (TMADPH fluorescence intensity

and specific turbidity calculated from the static light-scattering data).

Finally, changes in the secondary and tertiary structure of the DNA in lipoplexes were assessed by circular dichroism (CD) spectroscopy as a function of the sequence of mixing DNA and liposomes together. B-type is the natural form of plasmid DNA. Upon interaction with cationic liposomes the secondary DNA structure changed from B-type to a partial C-type due to dehydration and condensation of the DNA in lipoplexes [20]. Above a DOTAP/DNA mole ratio of 1.0, the DNA helices will be partially orientated in parallel to form a tertiary structure referred to as ψ-DNA [20]. In the present study, comparing curves 1 and 3 in Fig. 8A,B, we show that these changes in the secondary and tertiary structure of DNA were reversible and independent of the sequence of mixing during the preparation of lipoplexes (DNA added to liposomes, or vice versa; compare curve 1 in Fig. 8A with curve 2 in Fig. 8B).

4. Discussion

4.1. General

The main objective of this study was to investigate the relationships among defined physical properties of spontaneously formed DOTAP-containing lipoplexes (level of charge neutralization, size and lamellarity, size instability, and DNA structure), mode of lipoplex formation, and lipofection efficiency in vitro. For a more in-depth insight into these relationships, we also studied the extent of reversibility in the parameters which defined plasmid DNA–cationic liposome interaction and lipofection efficiency. To overcome complications in the analysis due to the effects of cell type, medium, the specific cationic lipid, and the plasmid, we focused on one cationic lipid which is commonly used for lipofection (DOTAP) in a defined medium using for lipofection one type of cells (NIH-3T3) and one plasmid (pS16-hGH). Transfection efficiency was quantified by measuring level of hGH in the cell medium. The variables under investigation were the absence or presence and the type of helper lipid (comparing DOPE and DOPC), DOTAP to DNA charge ratio, lamellarity of the cationic liposomes, and the order of mixing the plasmid DNA and the cationic liposomes (adding plasmid DNA to cationic liposomes or vice versa, and lipoplex preparation in one or two steps).

The results of this study point out that lipoplexes should be physicochemically characterized at two different levels of the structure: the macro level which relates to size and size instability; and the micro level which relates to the intimate interaction between the plasmid DNA and the lipids. Determining to what extent each of these two structure levels is involved and contributes to the lipofection process may be an informative approach to evaluate lipofection.

In this discussion section, the results will be examined and evaluated with respect to the concept of macro and micro structure of the lipoplexes.

4.2. Lipofection efficiency

We confirm many previous observations [6,21,22] that helper lipids improve lipofection efficiency of lipoplexes (see Figs. 1 and 2). Many studies suggest that phosphatidylethanolamine (and especially DOPE) is the preferred helper lipid for in vitro lipofection. However, this issue of the optimal helper lipid remains controversial since in one study DOPC performs better [23], while in another study cholesterol was superior to phospholipids [24]. Our studies, when combined with those of others described above, suggest that the situation is probably dependent, to a large extent, on the cell type. We found that differences between DOTAP/DOPE (1:1) mediated transfection and DOTAP/DOPC (1:1) mediated transfection were small (the only large difference was found when the plasmid DNA was added to MLV at a DNA/DOTAP charge ratio of 0.2). This similarity was unaffected by the lamellarity of the liposomes used for complexation with the DNA or by the DNA/cationic lipid ratio (compare Figs. 1 and 2). However, a significantly lower transfection efficiency was found in the lack of helper lipid (100% DOTAP) except at the low DNA/DOTAP ratio of 0.2. Then, the 100% DOTAP mediated transfection was as efficient as, or better than, the DOTAP/DOPE (1:1) mediated transfection for MLV (Fig. 1) and LUV (Fig. 2). Increasing the incubation time of the lipoplexes before their addition to the cells resulted in a slight decrease in transfection efficiency (Fig. 3). This might be caused by aggregation of the lipo-

plexes or by desorption of DOTAP out of the lipoplexes due to its high critical aggregation concentration of 7×10^{-5} M [17].

4.3. MLV versus LUV as starting reagent for lipoplex formation

Many studies (see below) have been performed in order to compare multilamellar with unilamellar liposomes as a starting reagent for lipoplex formation. Multilamellar vesicles are much less homogeneous, but much easier to prepare [25]. Large unilamellar vesicles ($\sim$100 nm) have the advantage of being much more homogeneous with respect to size distribution than MLV and therefore they are also easier to sterilize and to characterize. This makes LUV superior to MLV as pharmaceuticals. Also, larger mole fractions of their lipids are exposed to immediate interaction with the DNA.

The issue of MLV versus LUV (or SUV) is controversial [26]. Our data agree with those of Liu et al. [24], Yagi et al. [27], and Felgner et al. [22] and Zelphati et al. [34], which show that the transfection efficiencies were in general higher when plasmid DNA was mixed with MLV than with LUV (compare Figs. 1 and 2). We also demonstrate that MLV transfection efficiency is less dependent on DNA/DOTAP concentration than that of LUV. Similar results were obtained for DOTAP/DOPC and DOTAP/Chol liposomes (data not shown). Therefore, due to the combination of simplicity and superiority in transfection, MLV should be preferable for lipoplex formation.

The data by Templeton et al. [28] which show superiority of LUV seem contradictory to the above [22,24,27], but they cannot be compared with those previous data, including ours, in which the lipoplexes were formed spontaneously and used as such. Templeton et al. [28] did not use spontaneously formed lipoplexes, but modified them by a combination of ultrasonic irradiation and low pressure extrusion to a LUV in which the DNA is encapsulated. It is important to note that while for MLV the optimal DNA/DOTAP ratio was 0.2, for LUV it was 0.5. This may be related to the fact that in LUV more lipid molecules are exposed for first contact with DNA and therefore more DNA is required to reach the optimal ratio.

4.4. Mode of DNA–cationic liposome interaction

We concentrated on DNA–DOTAP/DOPE (1:1) lipoplexes and studied their physicochemical properties and lipofection under various modes of preparation at a broad range of DNA/DOTAP charge ratios. The lipophilic fluorophores HC and TMADPH were used to monitor DOTAP electrical neutralization [17,19] and changes in membrane defects [18]. Static light-scattering (specific turbidity) of lipoplexes was used to measure relative size changes and size stability [17–19]. CD spectroscopy of DNA in lipoplexes was used to follow changes in DNA secondary and tertiary structure [20]. The estimation of the dissociation degree of HC in a buffered solution allows the determination of the electrostatic properties of the lipid surface [19]. We demonstrated that interaction between the negatively charged plasmid DNA and the cationic lipids caused a neutralization of the positive charges of the lipids, which was monitored by HC 380/330 nm fluorescence ratio. Previously [19], we showed an almost 1:1 correlation between the dissociation degree of HC in the assembly containing cationic lipid and the percentage of remaining positively charged lipids in this system. The results describing the properties of spontaneous lipoplexes formed during the course of the two-step mixing between the plasmid DNA and the cationic liposomes are very informative in explaining the mechanism of lipoplex formation and stability. They point out that the changes of neutralization, lipid packing, and level of defects in lipid packing of the lipid in the lipoplexes by the plasmid DNA are close to being fully reversible (Figs. 5 and 7 and Table 1) and are dependent mainly on the DOTAP/DNA charge ratio at any given step of the mixing and not on the order of mixing, the lamellarity of the vesicles, or the number of mixing steps. Similarly, the change in the secondary and tertiary structure of the plasmid DNA ($B\rightarrow$partial C helix transformation and ψ^--structure, respectively) were reversibly modified and controlled mainly by the DNA/DOTAP charge ratio (Fig. 8). This suggests that at the level of charge neutralization (the main thermodynamic driving force for lipoplex formation [10]), the interaction between plasmid DNA and the cationic lipids is almost instantaneous and fully reversible.

Due to this reversibility, a classical phase diagram

can be constructed, in which can be analyzed the B→partial C change in DNA structure, which involves changes between a higher and a lower level of DNA hydration, and the appearance and level of spatial arrangement of the plasmid DNA associated with the lipid bilayer (as determined from the level of ψ^--structure). While at the level of the microstructure, DNA–DOTAP interaction is reversible, this is not the case for the macrostructure. It seems that once the lipoplexes reach a high level of size instability due to lipid packing defects (DNA/DOTAP charge ratio of excess cationic lipid ($\sim$0.5)), they reach an irreversible stage with respect to size. The history of obtaining this ratio does not matter, but once it is reached, size becomes large and remains so (Fig. 7 and Table 1).

Another important implication of the reversibility in neutralization and changes in DNA structure is that most of the time DNA must be available to the lipid molecules, which supports the claims of Eastman et al. [29] that in lipoplexes formed spontaneously in this range of charge ratios (DNA/DOTAP 0.2–2.0) most DNA (although condensed) is actually exposed and not encapsulated by a lipid bilayer. In this respect, the spontaneously formed lipoplexes described here differ from lipoplexes formed non-spontaneously, i.e. with energy input [28]. The differences in size between spontaneously and non-spontaneously formed lipoplexes, size stability, shape, and exposure of plasmid DNA are expected to have major implications for lipofection efficiency, especially in vivo [28].

Surprisingly, lipofection followed the macrostructure and not the microstructure. In a way, it seems that when the lipoplexes pass through a stage that their DNA/DOTAP charge ratio is 0.5, then even if the ratio is later increased to 2.0, they will 'remember' the lower ratio and their lipofection efficiency will be much closer to that at the DNA/DOTAP ratio of 0.5 than to the ratio of 2.0 (Fig. 4). However, if the lipoplexes were formed at a DNA/DOTAP ratio of 2.0 and then shifted to a ratio of 0.5, the lipofection efficiency again will be closer to that achieved at a ratio of 0.5 (one-step mixing, Fig. 4).

One of the striking aspects of the DNA/DOTAP charge ratio of 0.5 is the great instability in size [18,19], which results from membrane defects due to lateral phase separation between regions of bilayers which were condensed by DNA and those which were not [18]. It is still unknown what level of instability is required for optimal transfection. Possibly, the superiority of MLV over LUV for lipoplex formation may suggest that dependence of lipofection on the level of instability has a bell-shaped curve. Based on structural considerations, the level of cationic lipid exposure to DNA in MLV will be smaller, which at low DNA/DOTAP charge ratio will lead to a smaller number of defects per liposome. This is supported by the fact that size changes for MLV were smaller than those observed for LUV (Fig. 6). Similarly, such an optimal ratio may also explain the superiority in lipofection efficiency of adding LUV to DNA over the addition of DNA to LUV (Fig. 3). Lipoplex populations are heterogeneous with respect to many physicochemical parameters, including size, structure at the molecular level, and dynamics (both assessed by P NMR [30]). They are also heterogeneous in lipofection efficiency [30]. It can be assumed that lipofection efficiency is related to the fraction of a specific population of lipoplexes. Mok and Cullis [30] propose that this fraction consists of those lipoplexes having a large level of non-bilayer lipid structure. Koltover et al. [31] suggest that the inverted hexagonal phase is the important factor. However, many studies show that there are other alternatives to efficient lipofection, as helper lipids which do not support an inverted hexagonal phase, or non-bilayer structures, such as cholesterol, also improve lipofection to a large extent [24,35]. Therefore, we propose that defects in lipid packing (which can be introduced by various means) which lead to inherent instability are the common denominator for optimizing lipofection.

Another important aspect of the reversibility of all parameters related directly to the intimate interaction between DNA and lipids (which defined the microstructure of the lipoplex) is that the addition or removal of lipid components, such as acidic lipids [32] or cationic lipids, having high critical aggregation concentration (CAC) [17] may lead to lipoplex dissociation [32,33] which is obligatory for efficient transfection.

Finally, there is the issue of correlation between the transfection efficiencies in vitro and in vivo [4]. Needless to say, the in vivo transfection is a much more complicated process than the in vitro transfec-

tion, especially when the spontaneously prepared lipoplexes are administrated intravenously, as these lipoplexes face many obstacles which do not exist in the in vitro process. These obstacles include interactions with serum components which modify the structure and properties of the spontaneous lipoplexes ([35,36] and reviewed in [4]) and are therefore expected to affect transfection. In addition, lipoplexes before and/or after modifications may interact with white blood cells and blood vessels in a 'non-productive' way which will dramatically reduce transfection efficiency. We are now in the process of applying the approach described in this paper to characterize changes that occur in lipoplexes in various body fluids and whole blood. With this knowledge, one can hope to design lipoplexes which will resist or minimize in vivo induced changes in them. Preliminary encouraging steps in this direction are presented in the study of the late Papahadjopoulos and coworkers [35] which demonstrate that replacing DOPE in the spontaneous lipoplexes (which induce hexagonal II phase in serum) by cholesterol (which does not have such an effect) improves the transfection in vivo dramatically, while in vitro, DOPE was somewhat superior to cholesterol as a helper lipid. A different approach was to replace spontaneous lipoplexes by non-spontaneous lipoplexes [28] which may be less affected by various factors present in body fluids. Inclusion of steric barriers at the level that will not stop the interaction of lipoplexes with the target cells is another promising approach [35]. However, in order to understand what affects the transfection efficiency a thorough characterization of the lipoplex is a prerequisite.

Acknowledgements

We would like to thank Dr. O. Meyuhas of our department for the gift of the *Escherichia coli* containing the plasmid pS16-GH and the NIH-3T3 cells, and we gratefully acknowledge the financial support by the Valazzi-Pikovsky Fellowship Fund to N.J.Z. and by the Israel Science Foundation to Y.B. (Grants 494/96 and 8004/98).

References

[1] J.S. Remy, C. Silin, J.P Behr, in: J.R.S. Phillippol, F. Schuber (Eds.), Liposomes as Tools in Basic Research and Industry, CRC Press, Boca Raton, FL, 1995, pp. 159–170.
[2] P.L. Felgner, Y.J. Tsai, J.H. Felgner, in: D.D. Lasic and Y. Barenholz (Eds.), Handbook of Nonmedical Applications of Liposomes, Vol. 4, CRC Press, Boca Raton, FL, 1996, pp. 43–56.
[3] D.D. Lasic, N.S. Templeton, Adv. Drug Deliv. Rev. 20 (1996) 221–226.
[4] D.D. Lasic, Liposomes in Gene Delivery, CRC Press, Boca Raton, FL, 1997.
[5] L. Huang, J. Liposome Res. 7 (1997) 143–220.
[6] X. Zhou, L. Huang, Biochim. Biophys. Acta 1189 (1994) 195–200.
[7] K. Goyal, L. Huang, J. Liposome Res. 5 (1995) 49–60.
[8] J. Zabner, A.J. Fasbender, T. Moninger, K.A. Poellinger, M. Welsh, J. Biol. Chem. 270 (1995) 18997–19007.
[9] S.W. Hui, M. Langer, Y.L. Zhao, P. Ross, E. Hurley, K. Chan, Biophys. J. 71 (1996) 590–599.
[10] S. May, A. Ben-Shaul, Biophys. J. 73 (1997) 2427–2440.
[11] D. Harries, S. May, W.M. Gelbart, A. Ben-Shaul, Biophys. J. 75 (1998) 159–173.
[12] F.D. Ledley, Pharm. Res. 13 (1996) 1595–1614.
[13] S. Levy, D. Avni, N. Aariharan, R.P. Perry, O. Meyuhas, Proc. Natl. Acad. Sci. USA 88 (1991) 3319–3323.
[14] Y. Barenholz, S. Amselem, in: G. Gregoriadis (Ed.), Liposome Technology, Vol. I, 2nd edn., CRC Press, Boca Raton, FL, 1993, pp. 527–616.
[15] T. Maniatis, E.F. Fritsch, J. Sambrook, Molecular Cloning. A Laboratory Manual, Cold Spring Harbor Laboratory, Cold Spring Harbor, NY, 1982.
[16] R.C. MacDonald, R.I. MacDonald, B.P.M. Menco, K. Takeshita, N.K. Subbarao, L. Hu, Biochim. Biophys. Acta 1061 (1991) 297–303.
[17] N.J. Zuidam, Y. Barenholz, Biochim. Biophys. Acta 1329 (1997) 211–222.
[18] D. Hirsch-Lerner, Y. Barenholz, Biochim. Biophys. Acta 1370 (1998) 17–30.
[19] N.J. Zuidam, Y. Barenholz, Biochim. Biophys. Acta 1368 (1998) 115–128.
[20] N.J. Zuidam, A. Minsky, Y. Barenholz, submitted for publication.
[21] E. Brunette, R. Stribling, R. Debs, Nucleic Acid Res. 20 (1992) 1115.
[22] J.H. Felgner, R. Kumar, S.H. Sridhar, C.J. Wheeler, Y.J. Tsai, R. Border, P. Ramsey, M. Martin, P.L. Felgner, J. Biol. Chem. 269 (1994) 2550–2561.
[23] C. Ho, C.D. Stubbs, Biophys. J. 63 (1992) 897–902.
[24] Y. Liu, L.C. Mounkes, H.D. Liggitt, C.S. Brown, I. Solodin, T.D. Heath, R.J. Debs, Nat. Biotechnol. 15 (1997) 167–173.
[25] D. Lichtenberg, Y. Barenholz, Methods Biochem. Anal. 33 (1988) 337–462.

[26] M.J. Bennet, A.M. Aberle, R.P. Balasubramaniam, J.G. Malone, M.H. Nantz, R.W. Malone, J. Liposome Res. 6 (1996) 545–565.
[27] K. Yagi, H. Noda, M. Kurono, N. Ohishi, Biochem. Biophys. Res. Commun. 196 (1993) 1042–1048.
[28] N.S. Templeton, D.D. Lasic, P.M. Frederik, H.H. Strey, D.D. Roberts, G.N. Pavlakis, Nat. Biotechnol. 15 (1996) 647–653.
[29] S.J. Eastman, C. Siegel, J. Tousignant, A.E. Smith, R.K. Cheng, R.K. Scheule, Biochim. Biophys. Acta 1325 (1997) 41–62.
[30] K.W.C. Mok, P.R. Cullis, Biophys. J. 73 (1997) 2534–2545.
[31] I. Koltover, T. Sasldit, J.O. Radler, C.R. Safinia, Science 281 (1998) 78–81.
[32] F.C. Szoka, Y. Xu, O. Zelphati, J. Liposome Res. 6 (1996) 567–587.
[33] P. Harvie, F.M.P. Wong, M.B. Bally, Biophys. J. 75 (1998) 1040–1051.
[34] O. Zelphati, C. Nguyen, M. Ferrari, J. Felgner, Y. Tsai, P.L. Felgner, Gene Ther. 5 (1998) 1272–1282.
[35] B. Sternberg, K. Hong, W. Zheng, D. Papahadjopoulos, Biochim. Biophys. Acta 1375 (1998) 23–25.
[36] O. Zelphati, L.S. Uyechi, L.G. Barron, F.C. Szoka Jr., Biochim. Biophys. Acta 1390 (1998) 119–133.